Development Challenges of Brain Functional Monitoring using Untethered Broadband Frequency Modulated fNIR System

K. Manseta, E. Sultan, A. M. Khwaja, K. Pourrezaei[+], A. Joshi[#], L. Najafizadeh*, A. Gandjbakhche*, A. S. Daryoush

Department of ECE, Drexel University, Philadelphia, PA 19104 USA
[+]School of Biomedical Engineering and Health Systems, Drexel University, Philadelphia, Pennsylvania 19104, USA
[#]Discovery Semiconductors, Inc. 119 Silvia St., Ewing, NJ 08628, USA
[*]National Institutes of Health, 9000 Rockville Pike, Bethesda, Maryland 20892 USA
Corresponding author: daryoush@ece.drexel.edu

***Abstract*- Spectroscopic measurements of brain matter is considered at near infra-red region, where optical properties are characterized by the refractive index n, absorption coefficient μ_a, modified scattering coefficient μ'_s, and anisotropy factor g. Development of a free space optical system over broadband is optimized in terms of improved signal to noise ratio. The data collected by sensor is communicated to a remote processor using an ultra wideband communication system to provide wireless access and full mobility.**

I. INTRODUCTION

Brain imaging has been widely considered to monitor brain physiological activities and it is proposed as a transportable device for monitoring traumatic brain injuries (TBI). Since neuronal activity of brain requires oxygen, these activities could take form of blast injuries [1], emotional instability [2], or even thinking. Spectroscopic measurements of brain tissue at near-infrared wavelengths of 680nm, 780nm, 808nm, 850nm, and 980nm are a very active and accurate method to detect levels of oxygenated and de-oxygenated hemoglobin [3], which explain the functionality of the brain and could be applied for differentiation of tumor and cyst. The location and percentage of oxygen absorbed in the brain can be related to different physiological activities [4] and hence labeled as functional near-infrared (fNIR) system. Commercial systems are now being marketed by Honda [5] which are based on fiber optic technologies. These systems are tethered and are not field transportable. Moreover, the systems are designed based on narrowband operation, however, higher extraction accuracy has been demonstrated in broadband systems [6]. In addition a higher spatial resolution and sensitivity is measured at higher frequencies. Finally, the broadband operation allows extraction of multilayer tissue as diffused photon penetrates deeper in the tissue. This paper discusses design challenges and measured performance of a broadband (70-1000MHz) free space optical link that is integrated with ultra wideband (UWB) wireless communication system.

II. APPROACH

There are two ways of implementing an fNIR imaging system. One is through optical fibers and wired links, as demonstrated in [5]. Our approach is to use free space optics and wireless links as depicted in Fig. 1. The advantage of the second method is the reduction of wires which makes it more appealing to employ; however, in addition to small foot print optical transmitter and receiver modules, it requires a wireless communication board. Since for a free space optical system, focusing and light collection is critical, Gradient-Index (GRIN) lens is used in our system. The communication between the monitoring device and the sensor can be done using a wireless link.

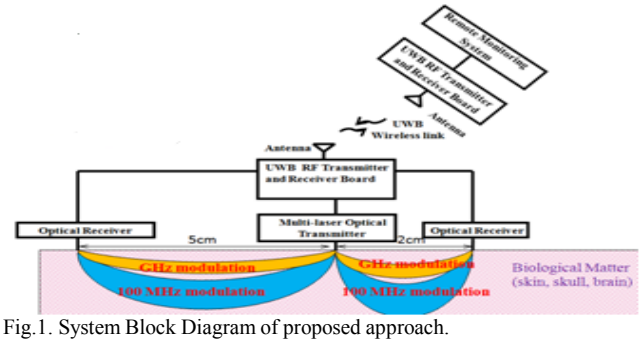

Fig.1. System Block Diagram of proposed approach.

A. Free Space Optical System vs. Fiber based system

At the detector, the light input from the tissue is scattered in all directions. To pick up maximum optical energy from the tissue, we need to use some focusing device. GRIN Lens is used in our system as a mechanism for light focusing. GRIN lens focus light through controlled radial variation of the refractive index from the optical axis to the edge of the lens. A comparison of light coupling efficiency is reported for GRIN lens versus different diameter plastic optical fibers [7]. It was found that coupling efficiency of GRIN lens is much better than that of plastic optical fiber. Typical diameter of 0.47 pitch GRIN lens optimized for performance at 808nm is 2 mm with length of 9.8 mm.

978-1-4244-7825-5/10/$26.00 ©2010 IEEE

Standard graded index profile of lens is used for performance comparison using commercial CAD tool (OSLO program) of GRIN lens against the large diameter optical fibers. The coupling efficiency of different diameters plastic fibers and GRIN lens was calculated. We found that the coupling efficiency of plastic fibers is between 17% (250µm in diameter) and 30% (1000µm in diameter) while for the GRIN lens coupling efficiency greater than 99% is measured. Thus GRIN lens gives us better focusing and light collection efficiency capability than even large plastic fibers. However GRIN lens is more sensitive to misplacement than the optical fiber.

B. Optical link Loss in Skull & Cortex

Diffusion Equation (DE) provides a sufficiently accurate description of light propagation in diffused media. Photons propagate in the diffusive media following a photon migrating banana shaped path from the source to the detector as represented in Fig. 1. The diffusion equation [8] is applied to calculate the insertion loss and insertion phase based on different scattering and absorption coefficients. The two important media that we are focusing on are skull and cortex. Most of the physiological changes will take place in the cortex, where oxygen is absorbed. The insertion loss and insertion phase of modulated NIR light through skull and cortex was simulated at different modulation frequencies. The relevant coefficients are presented in Table I for wavelength of 780nm and 850nm, but the representative results are plotted in Fig. 2 for 780nm.

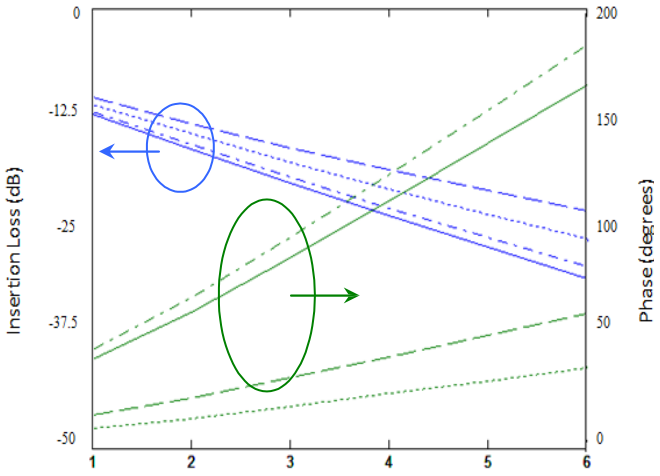

Fig. 2. Calculation plot of insertion loss and insertion phase vs source detector separation passing through skull (solid lines) and cortex (dash lines) at 141MHz (solid dot) and 1GHz (solid) modulating frequencies at optical wavelength of 780nm.

C. *Free Space Optical Link Analysis*

The overall direct modulation link performance is product of optical transmitter & receiver gains and the square of the link current transfer function [9]. The optical loss in the diffused medium is a result of scattering and absorption. The overall signal to noise performance of direct modulation link is dominated by the output noise power.

The optical intensity noise sources of optical transmitter are relative intensity noise (RIN) of semiconductor laser and thermal noise power of the optical transmitter that is calculated using the Nyquist theorem. Typical RIN value of -135dB/Hz is considered for VCSEL. The optical receiver noise are contributed by shot noise of the pin-photodiode, thermal noise of the optical receiver, and correlated noise contribution of any electrical amplifier employed as transimpedance amplifier. The total noise power at the output of the optical receiver is the sum of all these individual noise powers. In commonly used fiber optic fNIR system, avalanche photodiode (APD) are used as the sensitive photodiode in the optical receiver, which introduces the additional multiplication noise known as *'excess noise'* to the overall receiver noise. Since pin-photodiode combined with transimpedance amplifiers exhibit a lower noise power, those are preferred over APD in our approach.

TABLE I ABSORPTION AND MODIFIED SCATTERING PARAMETERS [7]

Medium	**Skull**		**Cortex**	
Parameter	**μ'_s**	**μ_a**	**μ'_s**	**μ_a**
780nm	0.9	0.05	0.91	<0.01
850nm	0.9	0.05	0.92	<0.01

The expected overall noise power in a lossy diffused medium (a diffused phantom, which is more lossy than brain with μ_a = 0.045/cm and μ'_s = 10/cm) with a transmitter and receiver separation of 2cm is depicted in Fig. 3. We observe that the thermal noise of transimpedance amplifier (with typical gain of 30dBΩ) in the receiver is the dominant over all the other noise sources. Shot noise of APD is 20 dB higher than the pin-photodiode due to the presence of excess noise.

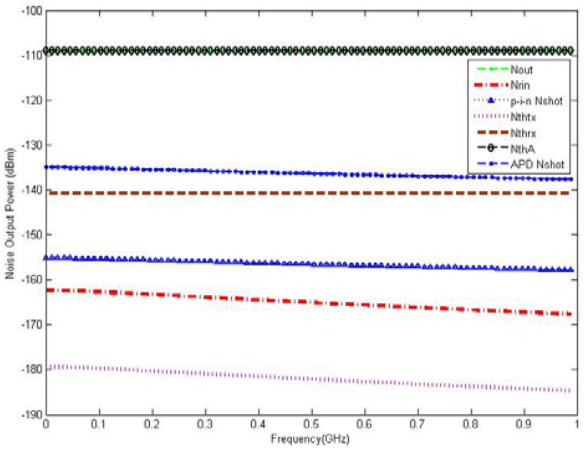

Fig. 3. Noise contribution to total noise output power vs frequency for APD and pin- photodiode based optical link through a diffused lossy medium.

SNR is defined as the ratio of the input power Pin times directly modulated optical link gain in diffused media over the total noise power. The input power is related to Irf as Pin= ½$|Irf|^2$Rj, where Rj is the laser junction resistance. Input RF current is limited by the full current swing, which is

limited at one end by threshold current (when laser is off) and the other end by maximum current (when laser is providing maximum reliable output optical power). From the simulation results, shown in Fig. 4, we observe a 5dB drop in the SNR with the increase in frequency. SNR of p-i-n receiver is same as the APD receiver due to the dominance of the transimpedance amplifier thermal noise.

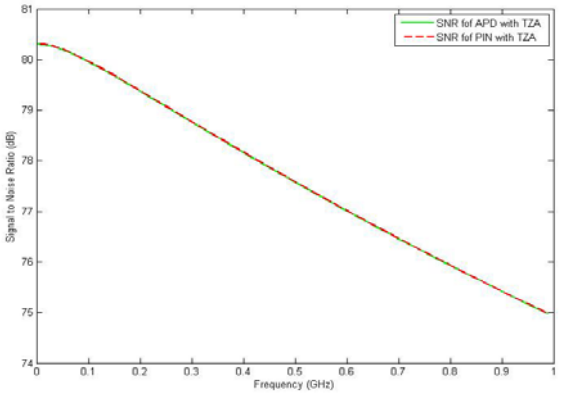

Fig. 4. Overall signal to noise ratio of the optical link as a function frequency.

III. FREE SPACE OPTICAL LINK REALIZATION

A. *Optical Transmitter*

The optical transmitter is responsible for transmitting photons into the diffused media. These photons will be either absorbed or scattered based on source detector separation, modulated frequency and laser intensity. In order to have all of these modulated parameters we need to have a transmitter that has the feature of frequency modulation and intensity modulation. The transmitter will perform as a microwave photonic modulator. Therefore, the designed and fabricated Optical Transmitter consists of dual wavelength vertical cavity semiconductor laser (VCSEL) diodes at two wavelengths of 780nm and 850nm (hereafter referred to as VCSEL A and VCSEL B, respectively). That will have the ability to transmit broadband RF power in frequency range of 70MHz to 1000MHz using a single-pull double through (SPDT) switch (Hittite HMC194). The Insertion Loss of the switch is 1.1dB and the Isolation is 23dB. The VCSELs used are capable of running at the speed of 2.5 Gb/s and packaged in TO-46. The equivalent circuit model packaged VCSEL mounted on a SMA connector is illustrated in Fig. 6. The leftmost stage represents the parasitic of the package leads, followed by the inductance and capacitance of the wire bonds of the package. The intrinsic VCSEL is modeled by a series resistance (representing the access resistance of the VCSEL) in shunt with a nonlinear capacitance Cj and resistance Rj (representing the p–n-junction diode capacitance as well as the distributed Bragg reflectors). A network analyzer with built in Bias-Tee, calibrated to the end of the microstrip line was used to measure the reflection (S_{11}) coefficient as a function of frequency and dc bias current. The measured VCSEL impedance magnitude and phase are fitted to this equivalent circuit model, for a bias current of 4.5mA.The values of the components for VCSEL-A are C_l=0.54pF,L_l=0.97nH, R_l=0.35Ω, Cp=0.28pF, L_p=1.90nH, L_c=0.14nH, R_s=43.09Ω, R_j=20.86Ω, C_j=15pF and for VCSEL-B C_l=0.19F, L_l=0.97nH, R_l=0.35Ω, Cp=0.52pF, L_p=1.15nH, L_c=0.12nH, R_s=44.96Ω, R_j=29.99Ω, C_j=13.3pF. The achieved agreement between the measured and simulated results is satisfactory in the frequency range from 0.1 MHz to 1.2 GHz.

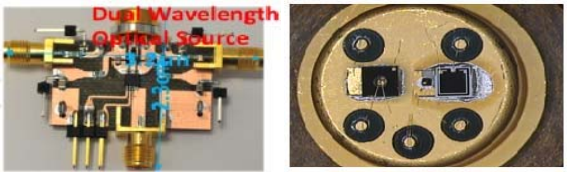

(a) (b)

Fig. 5. a) Dual wavelength laser driver with integrated SPDT Switch; b) Top view of VCSEL mounted in a TO-46 can.

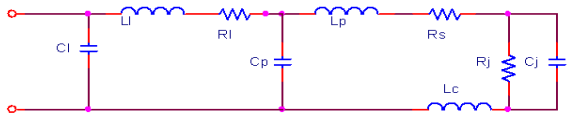

Fig. 6. Equivalent circuit model for VCSEL including device parasitic.

B. *Optical Receiver*

The receiver consists of HFD3180-203 which is a high-performance GaAs PIN photo-detector with very low junction capacitance. The detector has an efficiency of 0.5A/W. The pin-photodiode is followed by a low noise transimpedance amplifier with a gain upto 3kV/W. This detector is designed to meet performance requirements for data rates up to 4.25Gbps with a rise time of 80ps.

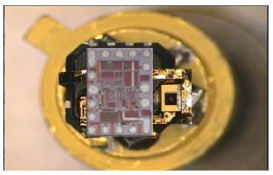

Fig. 7. Top view of photo-receiver with transimpedance amplifier chip.

C. *Link Measurement Results*

From the experimental results we see that the insertion loss of the optical link in free space is 21.7dB at 980 MHz. A flatness of 1dB is measured. The measured insertion loss is 20dB lower than the simulated value as no efforts were made to couple efficiently laser and detector since laser is to be placed on biological tissue. Using a GRIN lens will aid in focusing the transmitted light onto the photo detector and thus improve the optical link gain. The analysis and experimental results show that the gain and noise figure of the direct modulation optical link need to be improved by using laser and detector with higher electro- optic conversion efficiencies and better coupling efficiencies. As the desired operating bandwidth of the optical link is increased, the Q factors of the devices must be lowered according to Bode-Fano's theorem [10], and thus the transducer gains of the laser and detector circuits will degrade. Linear operation of a direct modulation optical link also depends largely on the ability to bias the laser diode away from the large-signal relaxation oscillation peak. To reduce the effect of thermal noise on total noise output power improvements should be made in the design of transimpedance amplifier by using a differential configuration.

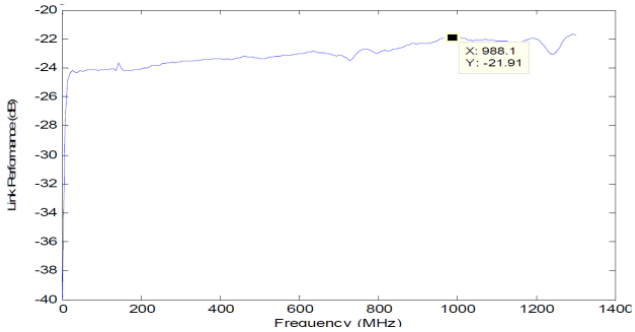

Fig. 8. Measured Link Loss vs Frequency

IV. UWB WIRELESS COMMUNICATION

The UWB Spectrum from 3.1GHz-10.6GHz is divided into 14 channels, each 528MHz wide [11]. We use channel 13 (9504MHz to 10032MHz) and channel 14 (10032MHz to 10560MHz) for our RF transmission. The baseband signal (IF) is from 30MHz to 1000MHz, the LO is at 9500MHz and the RF signal is from 9530MHz to 10500MHz. The transmitted power requirement for the UWB communications is -41.3dBm/MHz. Thus, for 1000MHz bandwidth, the transmitted power should be less than -11.3dBm. The wireless path loss is 60dB for 3m distance between transmitter and receiver. Thus the received signal is around -71.3dBm. A 20dB SNR will give us a BER of less than 10^{-6}. Thus to achieve this BER, we need the noise floor of the receiver to be less than -91.3dBm.

The RF input/output from/to antenna is down-/up- converted using the direct down/up conversion unit. Custom designed GCM (designed using InGaP HBT foundry services from Knowledge ON) is used for our system. The RF transmitter takes the baseband signal, up converts it using the custom built InGaP chip Gilbert Cell Mixer [12], amplifies the signal using Drive Amplifier, and transmits the amplified signal using an integrated Fractal Antenna. The RF Receiver takes the received signal from the Fractal Antenna, amplifies it using the low noise amplifier (LNA), and down converts it using the Gilbert cell mixer (GCM) into baseband signal. The measured conversion loss from such a device is around 11dB with 68dB.MHz$^{2/3}$SFDR.

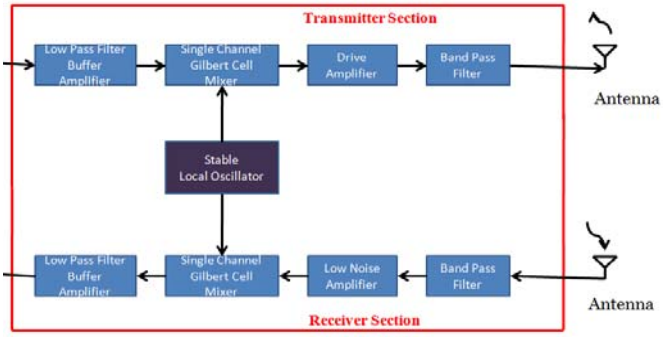

Fig. 9. RF Transceiver board with small size broadband fractal antennas

V. CONCLUSIONS

Design challenges of a free space optical fNIR system that its broadband frequency modulation employs untethered wireless communication are presented. A dual wavelength optical source with broadband pin-photodiode based optical receiver is implemented. The expected insertion loss and insertion phase of modulated NIR light through skull and cortex are simulated at different source and detector separations at two key modulation frequencies of 141 MHz and 1000MHz. Analytical results predict that the thermal noise of the transimpedance amplifier in the receiver dominates the total noise output which has been verified experimentally. A free space optical link has been realized with a dual wavelength laser and a high gain, low noise receiver. The measured insertion loss of the free space link was lower than the simulated value due to poor optical coupling, as the system is designed to be placed on biological tissue. While testing on the biological tissue, a GRIN lens will be placed with the optical receiver to aid in optical light collections and thus improve the optical link gain. The broadband modulating and demodulating signals are provided using UWB transceiver. Simulation results of the proposed free space optical link showed a very satisfactory agreement with the measurements.

VI. ACKNOWLEDGEMENT

This research is partly supported by the Center for Neuroscience and Regenerative Medicine (CNRM), and the Intramural Research Program (IRP) of Eunice Shriver National Institute of Child Health and Human Development (NICHD) of the National Institutes of Health.

REFERENCES

[1] Merzagora AC, Polikar R, Schultheis MT, Onaral B, "Combined fNIRS and EEG for the assessment of cognitive impairments following traumatic brain injury." Society of Applied Neuroscience Intl. Conf. 2008

[2] Irani F, Platek SM, Bunce S, Ruocco AC, Chute D, "Functional Near Infrared Spectroscopy (fNIRS): An Emerging Neuroimaging Technology with Important Applications for the Study of Brain Disorders." The Clinical Neuropsychologist, 21:9-37

[3] Villringer A, Dirnagl U., "Coupling of brain activity and cerebral blood flow: basis of functional neuroimaing", Cerebrovasc Brain Metab Rev. 1995 Fall;7(3):240-76.

[4] Yoko H, "Functional near-infrared optical imaging: Utility and limitations in human brain mapping", Psychophysiology, Volume 40 Issue 4, Pages 511 – 520

[5] http://www.hondanews.com/categories/1097/releases/4975

[6] Chenpeng Mu, Do Yoon Kim, Sunar. U, Pourrezaei K., Daryoush A.," Multi-wavelength NIR system for spectroscopy of biomedical tissues", Microwave Photonics proceeding, 2003. MWP, 275-278.

[7] http://www.globalspec.com/LearnMore/Optics_Optical_Components/Optical_Components/GRIN_Lenses

[8] Frédéric Bevilacqua, Dominique Piguet, Pierre Marquet, Jeffrey D. Gross, Bruce J. Tromberg, and Christian Depeursinge, "In Vivo Local Determination of Tissue Optical Properties: Applications to Human Brain", Applied Optics, Vol. 38, Issue 22, pp. 4939-4950 (1999).

[9] A. Daryoush, E. Ackerman, N. Samant, S. Wanuga and D. Kasemset, "Interfaces for high-speed Fiber-optic Links: Analysis and Experiments," IEEE Transactions on Microwave Theory and Techniques, vol. 39, no.12, December 1991.

[10] R. M. Fano, "Theoretical limitations on the broadband matching of arbitrary impedances," **J.** Franklin Inst., vol. 249, Jan.-Feb. 19.50, pp. 57-84 and 139-154.

[11] http://www.wimedia.org/en/index.asp

[12] A. M. Khwaja, P. Miranda, V. Mistry, C. Hinton, S. Garg, A. Sharma and A. S. Daryoush., "Ultra Wide Band System Realization for 4x4 MIMO Test Bed," IEEE Radio and Wireless Symposium, 2010. Pp 508-511.